Coordination of coupled electrified road systems and active power distribution networks with flexibility integration

(article starts on next page)

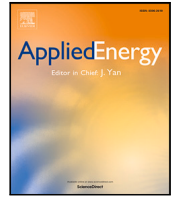# Coordination of coupled electrified road systems and active power distribution networks with flexibility integration

Arsalan Najafi [a,b], Georgios Tsaousoglou [c], Kun Gao [a,*], Omkar Parishwad [a]

[a] *Department of Architecture and Civil Engineering, Chalmers University of Technology, Gothenburg, SE 412 96, Sweden*
[b] *Department of Electrical Engineering Fundamentals, Wroclaw University of Science and Technology, 50-370 Wrocław, Poland*
[c] *Department of Applied Mathematics and Computer Science, Technical University of Denmark, Denmark*

ARTICLE INFO

ABSTRACT

Electric road systems (ERS) constitute a promising technology for mobile charging and relieving mandatory stops to recharge electric vehicles. However, the ERS operation is constrained by the limitations of the Power Distribution Network (PDN) that provides electricity. This study proposes a integrated optimization of a coupled ERS-PDN system (including traffic assignment and power flow modeling), in the presence of self-interested electric vehicle drivers, diverse flexibility resources and uncertainty of energy supplies (e.g. uncertainty from renewable energy). The security of the PDN while supporting ERS can be ensured by using active and flexible energy storage and flexible power loads. A semi-dynamic model is adopted for the traffic assignment. A stochastic bi-level optimization based on Stackelberg game under uncertainty is proposed to model the joint optimization problem to minimize the general cost of coupled ERS-PDN system and maximize the profit of the energy flexibility provider. Then, the Karush Kuhn Tucker conditions are deployed to convert the bi-level model to the equivalent single level model. The results demonstrate the effectiveness and benefits of the proposed framework using numerical experiments. The results show that the proposed optimization can reduce the burden of an ERS on the underlying PDN in improving the violated voltage by 3.66%, demonstrating the effect of joint consideration of diverse sources of flexibility.

1. Introduction

1.1. Background and research motivations

Electric vehicles (EVs) are recognized as sustainable alternatives for transportation due to their low emissions. As a matter of fact, EV markets exhibit exponential growth as sales exceeded 10 million in 2022. A total of 14% of all new cars sold were electric in 2022, and this percentage is expected to rise sharply in 2023 [1]. Nevertheless, the long charging times of EVs is a prominent disadvantage compared to diesel vehicles. The Electric Road System (ERS) technology holds the potential to offer a decisive solution to this obstacle. ERS is an electric road infrastructure system that can charge EVs through wireless charging technologies (overhead power lines and inductive charging technology), irrespective of the vehicle's motion and direction [2]. It allows EVs to eliminate the need to stop for recharging and saves time for charging as well [3]. Nonetheless, massive deployment of ERS creates new challenges. Massive ERS deployment combined with large traffic flow volume poses a significant increase in the required electricity

demands in power distribution networks (PDNs). The magnitude of this new load poses a major challenge for the PDNs' safe operation, which gives rise to the need for coordination between transportation systems and PDNs. Moreover, such coordination goes through socio-technical systems' considerations, as drivers are entitled to deliberately choose their route and generally opt for the one that offers them minimal overall travel cost (e.g., travel time and monetary costs) for their own trips [4]. Specifically, the users' selfish routing choices, if not accounted for, may result in unbalanced traffic flow distributions, which may consequently lead to an overload and voltage drop due to the high charging demands in some parts of the underlying PDNs.

Motivated by these challenges, this study proposes a novel framework to integrate flexibility in the operation of coupled ERS and active power distribution networks (APDN). The APDN refers to PDNs with a significant presence of controllable resources, e.g., vehicle-to-grid, battery energy storage, demand response services, and locally distributed generations (typically from renewable energies). Thereby, we consider a wireless ERS, the power of which is supplied through an

Nomenclature

A. Sets and indices

$t, \mathcal{T}$	Index and set of times.
$s, \mathcal{S}$	Index and set of scenarios.
$k, \mathcal{G}$	Index and set of DR utility companies.
$b, \mathcal{B}$	Index and set of nodes of active power distribution network.
$n, \mathcal{N}$	Index and set of nodes of the transportation system.
$\mathcal{B}^{\mathrm{N}}$	Set of electrified nodes of the active power distribution network.
$\mathcal{Z}_g$	Set of nodes of active power distribution network managed by gth DR provider.
$a, \mathcal{A}$	Index and set of links.
$d, \mathcal{D}$	Index and set of O–D pairs.
$k, \mathcal{K}$	Index and set of paths.
$j, \mathcal{J}$	Index and set of linear approximation segments.

B. Parameters

c_b	Investment cost of battery at b.
$D_{b,t}^{\mathrm{P}}, D_{b,t}^{\mathrm{Q}}$	Active and reactive loads of b at t.
$\pi_{t,s}^{\mathrm{M}}$	Electricity market price.
$\eta_b^{\mathrm{Ch}}/\eta_b^{\mathrm{Dc}}$	Charging/Discharging efficiency of battery.
$\overline{E}_b$	Upper bound state of charge of battery at b.
$\underline{E}_b$	Lower bound of the state of charge of battery at b.
$\mathrm{IFR}_y, \mathrm{ITR}_y$	Inflation and interest rate at the yth year of operation.
M_1, M_2	Big numbers.
NLC_b	Number of life cycle of battery at b.
$\overline{\mathrm{P}}_b^{\mathrm{Ch}}$	Upper bound of battery charge at b.
Γ_b	Curtailed power coefficient at APDN node b.
Θ_b	Curtailed energy coefficient at APDN node b.
$\overline{\mathrm{P}}_b^{\mathrm{Dc}}$	Upper bound of discharge of the battery at b.
PVF_b	Present value factor of battery at b.
r_b	Resistance of branch $b, b+1$.
$\overline{\mathrm{V}}, \underline{\mathrm{V}}$	Upper and lower bound of voltage.
x_b	Reactance of branch $b, b+1$.
$\overline{P}_{b,s,t}^{\mathrm{W}}$	Maximum generation limit of wind turbine b at t.
ρ_s	Probability of scenario s.
$\mathbb{I}_{akd}$	Link-path incidence binary matrix.
c_a	Traffic flow capacity at link a.
τ_a^0	Free travel time on link a.
Λ	Duration of time period.
$\overline{F}_{s,t}^d$	Traffic demand of O–D pair d.
$f^{\min}, f^{\max}$	Minimum and maximum traffic demand of paths.
$\tau^{\min}, \tau^{\max}$	Minimum and maximum residual time of traveling.
m_j^{slope}	Slope of segment j in piecewise approximation.
$\overline{x}_j$	Horizontal border of segment j.
$\overline{t}_j$	Vertical border of segment j.
T_a^C	Congestion toll on roads.

PF	Voltage deviation penalty factor.

C. Variables

$C_{g,s}^{\mathrm{DR}}$	DR cost of utility company g.
$C_{b,s,t}^{\mathrm{d}}$	Operation cost of battery at b in timeslot t.
$E_{b,s,t}$	Battery state of charge at b in t and s.
$P_{b,s,t}, Q_{b,s,t}$	Active and reactive power flowing through branch $b, b+1$ at t and s.
$P_{b,s,t}^{\mathrm{W}}, Q_{b,s,t}^{\mathrm{W}}$	Active and reactive generation through wind turbine b at t and s.
$P_{b,s,t}^{\mathrm{Ch}}/P_{b,s,t}^{\mathrm{Dc}}$	Charging and discharging power of battery at b in t and s.
$P_{b,s,t}^{\mathrm{LC}}$	Curtailment power of utility company g in APDN node b, at timeslot t and scenario s.
$P_{b,s,t}^{\mathrm{LS}}$	Shift power of utility company g in APDN node b, at timeslot t and scenario s.
$Q_{b,t}^{\mathrm{CAP}}$	Reactive power of capacitor banks at APDN node b at t and s.
$V_{b,s,t}$	Voltage magnitude of APDN node b at t and s.
$V_{b,s,t}^{\mathrm{DEV}}$	Voltage deviation from the minimum bound of APDN node b at t and s.
$\pi_{g,t,s}^{\mathrm{AG}}$	Offering price to DR utility company g at t and s.
$\varrho_{b,s,t}$	Binary variable to determine charging or discharging to the battery.
$P_{b,s,t}^{\mathrm{W}}$	Wind generation at APDN node b, timeslot t and scenario s.
$\tau_{a,s,t}$	Travel time on link a at t and scenario s.
$x_{a,s,t}$	Traffic flow on link a at t and scenario s.
$x_{a,s,t,j}^l$	Traffic flow on link a at t and scenario s of segment j.
$t_{a,s,t}'$	Traffic flow to power four on link a at t and scenario s.
$t_{a,s,t,j}^l$	Traffic flow to power four on link a at t, scenario s and segment j.
$f_{k,s,t}$	Traffic flow on path k, O–D d, at t and scenario s.
$u_{d,s,t}$	Minimal travel time of path k, at t and scenario s.
$\tau_{k,s,t}$	Residual travel time of path k, at t and scenario s.
$R_{s,t}^d$	Residual traffic demand of O–D pair d, at t and scenario s.
$F_{s,t}^d$	Modified traffic demand of O–D pair d at t and scenario s.
$U_{a,s,t,j}^x$	Binary variable associate with piecewise approximation segments.
$I_{k,s,t}$	Binary variable associate with Big-M method.

APDN with distributed resources (e.g. battery energy storage and small wind turbines). We envision a non-profit independent system operator that operates the coupled system of electric road systems and APDN. The APDN can use demand response (DR) flexibility, provided by the utility companies that represent electricity consumers. The envisioned framework is modeled as a bi-level Stackelberg game to capture the interaction of selfish DR providers and the independent system operator and to minimize the costs of the coupled ERS and APDN system. The following subsection describes the related works focusing on existing literature on the operation of coupled ERS and APDN.

1.2. Related works

The previous section motivated the co-optimization of traffic assignment in an ERS and efficient utilization of distributed flexibility connected to the underlying APDN. This section discusses the related work on each of the two systems as well as the few studies that consider a coupled system.

The EVs' long recharging times is deemed to be one of the main barrier to EV adoption [5]. This drawback motivates researchers and policymakers to investigate wireless ERSs as a promising, convenient, and safe solution. This innovative technology provides the infrastructure for EVs to charge wirelessly from roadbed transmitters while the vehicle is moving [6]. With emerging wireless ERSs, drivers should consider a recharging plan to choose a charging lane, the charging duration time, and the speed of an electric vehicle, as speed and travel time affect the amount of energy recharged [7]. The planning problem of locating wireless charging links and respective electricity prices was studied in [8], which also addresses the EV drivers' routing and recharging behavior to optimize the dynamic wireless charging system. In another planning effort, [9] suggested an approach to locate wireless charging facilities in an ERS, taking into account the objective of both sides, including transportation agencies and EV users, by considering the energy management cost and travel time. The planning of wireless charging infrastructure was also proposed in [10] for electric nodes, while the travel time and energy consumption uncertainties were addressed through a robust optimization method. Different energy consumption models were compared in [11] to obtain a strategy to investigate the quantitative effects of wireless ERSs on each EVs' link travel time. The above-discussed studies have not considered the electrical part and have disregarded the limitations posed by the underlying PDN that supports the ERS.

On the other hand, there are multiple studies that propose optimization frameworks from the APDN point of view. These studies typically consider EV charging stations (but not ERS) as an APDN flexibility resource. A generalized user equilibrium technique was proposed in [12] for coupled PDN and charging stations in electrified transport systems, where the possible paths were generated through a sub-problem by decomposing the main problem. The problem is scheduled for plugged-in EVs in a steady-state environment. An extension of the former paper can be seen in [13], where the proposed framework was extended to natural gas systems, including both EVs and gas-fueled vehicles. Additionally, the authors presented a coordinated planning approach for investment in both natural gas and charging stations. A similar endeavor was performed in [14] by extending the energy carriers to other types, e.g., cooling and heating, wherein the transportation system is one of the inputs of an energy hub. The fluctuation of nodal electricity prices significantly influences road congestion dynamics, particularly in proximity to charging station locations. [15] proposed a coordination approach to explore the solution of the coupled systems aiming at minimizing the operation costs of both ERS and PDN. In [16], the joint expansion planning of a PDN and transportation system was explored to find the best type, location, and capacity for roads, distribution lines, distributed generations, on-load tap changers, energy storage systems, and charging facilities. However, the study has focused on a static traffic assignment problem.

One of the main challenges in the coupled systems is the behavior modeling of EV owners. Generally, if drivers are rational, selfish, and have perfect information on traffic in the systems, the Wardrop equilibrium point will emerge. The authors in [17] studied the effects of the discrepancy between a path's perceived traveling cost and the actual traveling cost. There is a concern about the vulnerability of the coupled systems in extreme circumstances. To cope with disasters in coupled transport and distribution networks, [18] suggested several measures such as reversing the direction of roads, PDN line switching, and charging station pile management. The authors in [19] developed a model for coupled transportation and distribution networks as a

bi-level framework in the presence of wind power generation. The charging fee was modeled as the upper-level decision, and the traffic assignment problem was at the lower level. The resulting bi-level model was solved using a reinforcement learning approach. Moreover, instead of using a centralized optimization, [20] suggested a decentralized method to coordinate the PDN and electric transport systems. A model for dynamic coordination of the coupled transportation and distribution networks was developed in [21,22], in which the dynamic nature of the EV queue was taken into account in calculating traveling time. These works have considered coupled APDN and electrified transportation, with the coupling point being the EV charging stations (not ERS).

The development of wireless charging systems has led to a concentration on the coordination of PDNs and ERSs. One of the initial research in this coordination category was studied in [23] to investigate the coupled networks' static coordination (i.e. for a single point in time, without considering a horizon ahead). The coupled transport and distribution networks problem was also solved in [24] aimed at scheduling coupled networks using mobile energy storage. A combined static charging (with plug-in charging stations) and wireless charging was proposed in [25] to address both charging options at the same including the interdependency between PDNs and ERSs. The electricity prices were modeled through locational marginal prices, which means the prices change spatially, and consequently, it may change drivers' route choices. Although the electricity prices were addressed thoroughly, the technical impact of the ERSs on PDN was disregarded. A static coordination of two systems (PDN and ERSs) was proposed in [26] to define a bidirectional framework to sell or purchase electricity from EVs through wireless ERSs. A semi-dynamic approach was developed in [27] to coordinate the coupled problem concerning the residual dynamic flow and traveling time. While these works have considered coupled ERS and PDN systems, other power flexibility resources located at the PDN (and turning it into an APDN) were by and large disregarded, while the problem's temporal couplings were simplified or neglected.

Modeling and managing the APDN diverse power flexibility resources has been an active topic in the power systems' literature [28]. Accordingly, some studies have directed their attention toward the exploration of the flexibility in multi-energy storage devices, including electrical and thermal energy storage and their management with renewable energy resources and combined heat and power units [29]. Some research delved into the implementation of flexibility resources on a smaller scale, e.g., microgrids [30]. Naturally, in that literature, it is the transportation part that is typically neglected or, at best, simplified. The development of APDNs is served by recent advances in two-way communication capabilities. These capabilities have led to a significant increase in research on using flexibility advantageous, e.g., DR services and battery energy storage. Indicatively, the capability of EVs to support ancillary services, due to their temporal and spatial charging flexibility, quick response, and storage capability, was leveraged in [31] to coordinate the power transmission system operator and power distribution system operator (DSO). Similarly, EV charging/discharging flexibility was deployed in [32] to cope with the APDN's congestion and voltage problems. The flexibility of flexible loads and EVs was used in [33] and [34] to facilitate the coordination of neighboring APDNs and APDN energy management problems. An integrated unit comprising an electrical energy storage system and vehicle-to-grid (V2G), complemented by the demand response program, was suggested in [35] toward minimizing the difference between the expected energy cost and the expected profit of flexibility sources. These works used simplified models for EV charging stations and have abstained from modeling the routing and traffic assignment problem of EV drivers.

For better insight, Table 1 compares the included items in each reference. It should be noted that the "coupled system" given in the table indicates whether a reference has considered both PDNs and ERS (or a transportation system).

Table 1
Overview of the literature review and the including items in their approach.

Reference	Year	Traffic assignment problem	Coupled systems	Dynamic/semi-dynamic	ERS	Uncertainty	Demand response
[8]	2021	✓	✗	✗	✓	✗	✗
[9]	2020	✓	✗	✗	✓	✓	✗
[10]	2017	✓	✗	✓	✓	✓	✗
[11]	2018	✓	✗	✗	✓	✗	✗
[12]	2023	✓	✓	✗	✗	✗	✗
[13]	2022	✓	✓	✗	✗	✗	✗
[14]	2020	✓	✓	✗	✗	✗	✗
[15]	2023	✓	✓	✗	✗	✗	✗
[16]	2020	✓	✓	✗	✗	✓	✗
[17]	2022	✓	✓	✗	✗	✓	✗
[18]	2023	✓	✓	✓	✗	✗	✗
[19]	2020	✓	✓	✗	✗	✗	✗
[20]	2019	✓	✓	✗	✗	✗	✗
[21]	2023	✓	✓	✗	✗	✗	✗
[22]	2022	✗	✓	✓	✗	✗	✗
[23]	2017	✓	✓	✗	✓	✗	✗
[24]	2021	✓	✓	✓	✗	✓	✗
[25]	2020	✓	✗	✗	✓	✗	✗
[26]	2022	✓	✓	✗	✓	✗	✗
[27]	2020	✓	✓	✓	✓	✗	✗
[28]	2023	✗	✗	✓	✗	✓	✓
[29]	2023	✗	✗	✓	✗	✓	✗
[30]	2022	✗	✗	✓	✗	✓	✗
[31]	2022	✗	✗	✓	✗	✓	✗
[32]	2023	✗	✗	✓	✗	✓	✗
[33]	2023	✗	✗	✓	✗	✓	✓
[34]	2022	✗	✗	✓	✗	✗	✗
[35]	2022	✗	✗	✓	✗	✓	✓
Proposed method	–	✓	✓	✓	✓	✓	✓

1.3. Knowledge gap and contributions

The existing literature reveals valuable works in the coupled operation of distribution and transportation networks. However, there is a bold gap concerning the joint modeling and operation of the ERS's traffic assignment problem and the APDN energy management problem, especially in the presence of diverse flexibility resources and under uncertainty. Moreover, such a model should account for the self-interested behavior of the coupled system's users (including both EV drivers as well as electricity-providing utility companies). Finally, a comprehensive dynamic or semi-dynamic approach is needed to implement many temporal concepts and devices in APDNs, e.g., energy storage systems, demand response, vehicle to grid, etc.

To the best of our knowledge, such a comprehensive framework is modeled and solved for the first time in this paper. We use the semi-dynamic approach (which takes into account a 24-h look ahead) presented in [27] to address the dynamic nature of our coupled APDN and wireless ERS, which makes a trade-off between accuracy and complexity level. The current literature has mostly focused on studying a static time domain, which is not suitable for addressing the dynamic aspects of flexibility resources in APDNs. Then, we propose our framework to develop flexibility in the coupled coordination of APDN and ERS, including demand response services and battery energy storage. The flexibility can facilitate the operation of distribution networks, specifically during rush hour of traffic and electrical demands, which becomes more critical if we consider that traffic demands are a function of drivers' behavior and are big enough to endanger the security of the power distribution network. Flexible consumers can perform smart actions of load curtailment of load shifting when it is desired, whereas the battery employs energy arbitrage strategies to provide support during peak demand periods. Moreover, we also consider renewable energy resources as a major source of uncertainty, while accounting for the selfish behavior of profit-maximizing utility companies that manage the distributed resources. Besides, we tackle the uncertainties stemming from renewable energy generation, traffic demands, and electricity prices through stochastic programming, which have not been studied simultaneously so far.

The proposed model provides a better understanding of the couplings between the two systems and how diverse elements (e.g. a driver's routing preferences and a power utility company's profit-maximizing decisions) can affect one another.

1.4. Paper organization

We organize this paper as follows. First, we present the system model in Section 2, describing the mathematical models of the battery energy storage, the utility companies' decisions, the traffic assignment problem, and the power flow model. The solution methodology is given in Section 3 to address the proposed bi-level structure through convexification non-convexities. In Section 4, the results and discussion are provided, and finally, the conclusion is given in Section 5.

2. Modeling framework

We consider a coupled system (wireless ERS and APDN) operated within a time horizon $\mathcal{T}$. We are interested in minimizing the overall expected system's cost $\mathbb{E}[C]$ which comprises the (weighted) transportation system cost C^{ERS} and the electricity cost C^{APDN}, over a set S of discrete scenarios for the systems' uncertain parameters, as in:

$$\mathbb{E}[C] = \sum_{s \in S} \rho_s \cdot \left(\omega C_s^{\text{ERS}} + C_s^{\text{APDN}} \right). \tag{1}$$

where ω is the weight parameter that strikes the desired balance between the two different types of costs, and ρ_s is the probability of scenario s. The APDN system includes wind turbines, storage facilities as well as flexible consumers able to adjust their consumption in response to incentives. Fig. 1 provides a schematic overview of the system.

The ERS is defined over a set $\mathcal{N}$ of nodes and the set $\mathcal{A}$ of their interconnecting links (i.e. electrified roads), while the APDN is defined over a set $\mathcal{B}$ of nodes and their interconnecting power lines. The coupling between the two systems, stems from the fact that the traffic flow $x_{a,s,t}$ on road $a \in \mathcal{A}$, in timeslot $t \in \mathcal{T}$ and scenario $s \in S$ brings an analogous power consumption $P_{b,s,t}^{\text{ERS}} = \eta_a \cdot \mathbb{I}_{ab} \cdot x_{a,s,t}$ to node $b \in \mathcal{B}$ of the APDN, where η_a is road's traffic-flow-to-power-consumption conversion
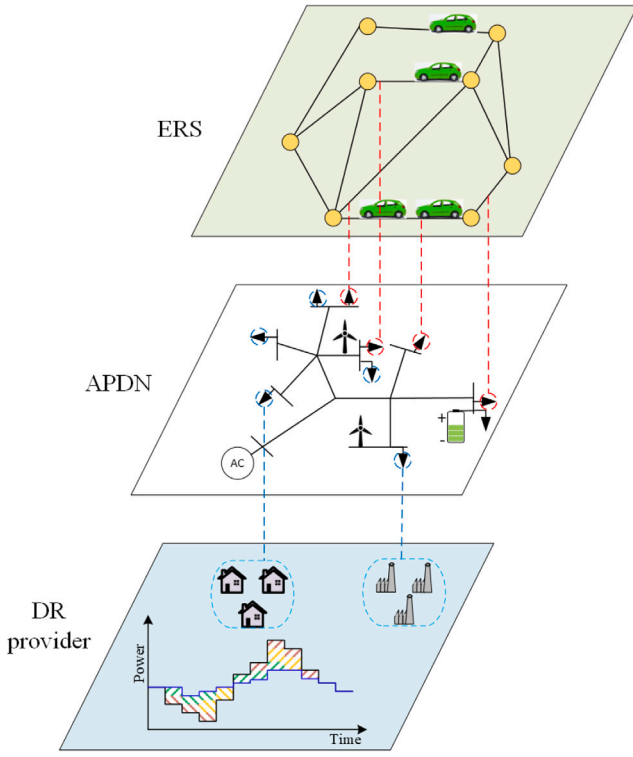
Fig. 1. Relation among the decision-making agents in the proposed framework.

factor, and $\mathbb{I}_{ab}$ is the indicator function which is equal to one if road $a \in \mathcal{A}$ is powered by node $b \in \mathcal{B}$, and zero otherwise.

Each system has its own set of variables, denoted as $\mathcal{V}_{s,t}^{\mathrm{ERS}}$ (for the ERS system) and $\mathcal{V}_{s,t}^{\mathrm{APDN}}$ (for the APDN system), as well as its own set of feasible operational points $\mathcal{F}^{\mathrm{ERS}}$ and $\mathcal{F}^{\mathrm{APDN}}$ defined by a set of (non-coupling) constraints. Thus, our high-level objective takes the form of the following cost-minimization problem:

$$\min \left\{ \sum_{s \in S} \rho_s \cdot \left(C_s^{\mathrm{ERS}} + C_s^{\mathrm{APDN}} \right) \right\}$$

$$\mathbf{over} \ \left(\mathcal{V}_{s,t}^{\mathrm{ERS}} \cup \mathcal{V}_{s,t}^{\mathrm{ERS}} \right)_{s \in S, t \in \mathcal{T}}$$

$$\mathbf{subject\,to} :$$

ERS constraints: $\mathcal{V}_{s,t}^{\mathrm{ERS}} \in \mathcal{F}^{\mathrm{ERS}}, \quad \forall t \in \mathcal{T},$

APDN constraints: $\mathcal{V}_{s,t}^{\mathrm{APDN}} \in \mathcal{F}^{\mathrm{APDN}}, \quad \forall t \in \mathcal{T},$

Coupling constraints: $P_{b,s,t}^{\mathrm{ERS}} = \eta_a \cdot \mathbb{I}_{ab} \cdot x_{a,s,t},$

$$\forall a \in \mathcal{A}, b \in \mathcal{B}, s \in S, t \in \mathcal{T}. \quad (2)$$

In the subsections to follow, we define the variables, constraints, and cost functions of each system in more detail.

2.1. ERS model

If we consider the rationality of EV users, the traffic pattern highly depends on two factors: the convenience of the drivers, and other vehicles' choices. Drivers prefer to choose paths with minimum travel time for convenience. On the other hand, since the travel time depends on the total traffic flow, the choice of drivers also depends on those of the other vehicles. Thus, traveling on the shortest path may not necessarily yield the shortest travel time because that path rapidly becomes congested when everyone opts for it simultaneously [4]. Thereupon, the two aspects mentioned motivate the modeling of travel time and user equilibrium, both of which should be addressed in the traffic flow model to be presented.

For the ERS $(\mathcal{N}, \mathcal{A})$, let $\mathcal{D} \subset \mathcal{N}^2$ denote the set of all relevant pairs (n_o, n_d) of origin–destination nodes, where $n_o, n_d \in \mathcal{N}$. Also, let $\mathcal{K}_d$ denote the set of paths that connect the origin–destination pair $d = (n_o, n_d) \in \mathcal{D}$.

The cost C_s^{ERS} of the system in scenario s is the product of the travel time $\tau_{a,s,t}$ and traffic flow $x_{a,s,t}$ across time of all road segments, i.e.:

$$C_s^{\mathrm{ERS}} = \sum_{a \in \mathcal{A}} \sum_{t \in \mathcal{T}} \tau_{a,s,t} x_{a,s,t}, \quad \forall s \in S. \quad (3)$$

where $\tau_{a,s,t}$ denotes the travel time of road segment a. The traveling time itself, depends on the flow due to congestion. This is modeled by the widely used Bureau of Public Roads function [36]

$$\tau_{a,s,t} = \tau_a^0 \left(1 + 0.15 \left(\frac{x_{a,s,t}}{c_a} \right)^4 \right), \quad \forall a \in \mathcal{A}, s \in S, t \in \mathcal{T}. \quad (4)$$

In turn, traffic on road a is comprised of the traffic caused by all paths $k \in \mathcal{K}_d, d \in \mathcal{D}$ that contain road a. This is captured by defining the traffic flow on path k as $f_{k,s,t}$ and setting

$$x_{a,s,t} = \sum_{d \in \mathcal{D}} \sum_{k \in \mathcal{K}_d} f_{k,s,t} \mathbb{I}_{akd}, \quad \forall a \in \mathcal{A}, s \in S, t \in \mathcal{T}, \quad (5)$$

where the indicator function $\mathbb{I}_{akd}$ is one if road a belongs to path k of pair d, and zero otherwise. The total travel time $\tau_{k,s,t}$ across path k is the sum of travel times across all roads of the path, i.e.:

$$\tau_{k,s,t} = \sum_{a \in \mathcal{A}} \tau_{a,s,t} \mathbb{I}_{akd}, \quad \forall s \in S, t \in \mathcal{T}, k \in \mathcal{K}_d, d \in \mathcal{D}. \quad (6)$$

The total traffic $F_{d,s,t}$ on pair $d \in \mathcal{D}$ is defined by the traffic on all paths $k \in \mathcal{K}_d$, as in

$$F_{d,s,t} = \sum_{k \in \mathcal{K}_d} f_{k,s,t}, \quad \forall d \in \mathcal{D}, s \in S, t \in \mathcal{T}. \quad (7)$$

We assume an admission policy where, for a pair $d \in \mathcal{D}$, the admitted traffic $F_{d,s,t}$ at t is a function of the pair's residual traffic $R_{d,s,t}$ and $R_{d,s,t-1}$ (for the present and previous timeslot respectively), as in

$$F_{d,s,t} = \widehat{\mathrm{F}}_{d,s,t} + \frac{1}{2} R_{d,s,t-1} - \frac{1}{2} R_{d,s,t}, \quad \forall d \in \mathcal{D}, s \in S, t \in \mathcal{T}, \quad (8)$$

where $\widehat{\mathrm{F}}_{d,s,t}$ is the traffic demand for d at s,t (i.e. a random variable) and $R_{d,s,t}$ is the residual traffic defined by

$$R_{d,s,t} = \sum_{k \in \mathcal{K}_d} f_{k,s,t} \frac{\tau_{k,s,t}}{\Lambda}, \quad \forall d \in \mathcal{D}, s \in S, t \in \mathcal{T}, \quad (9)$$

where Λ is the maximum travel times of all used paths, such that as the ratio $\frac{\tau_{k,s,t}}{\Lambda} \leq 1$ grows on a given path, more residual traffic is created.

Based on this subsection's formulations, the variables of the ERS are

$$\mathcal{V}_{s,t}^{\mathrm{ERS}} = \left(C_s^{\mathrm{ERS}}, \left(\tau_{a,s,t}, x_{a,s,t} \right)_{a \in \mathcal{A}}, \right.$$

$$\left. \left(F_{d,s,t}, R_{d,s,t}, \left(f_{k,s,t}, u_{d,s,t} \right)_{k \in \mathcal{K}_d} \right)_{d \in \mathcal{D}} \right), \quad (10)$$

$$\forall s \in S, t \in \mathcal{T},$$

and the set of feasible operational points $\mathcal{F}^{\mathrm{ERS}}$ is defined by the constraints (3)–(9).

It should be noted that, because the travel cost is minimized in the objective function, the resulting traffic management decisions are *implementable* in the sense that they are in line with the selfish routing preferences of the drivers who deliberate on the choice of their path. More specifically, assuming that a driver on route $k \in \mathcal{K}_d, d \in \mathcal{D}$ chooses the path with the lowest travel time, let us denote the lowest travel time among paths $k \in \mathcal{K}_d$ for a route $d \in \mathcal{D}$ as $u_{d,s,t}$. Then, the implementability property demands that traffic flows should satisfy the Wardrop equilibrium condition

$$0 \leq f_{k,s,t} \perp (\tau_{k,s,t} - u_{d,s,t}) \geq 0,$$

$$\forall k \in \mathcal{K}_d, d \in \mathcal{D}, s \in S, t \in \mathcal{T}. \quad (11)$$

2.2. Power flow model

We consider a radial APDN where a node $b \in \mathcal{B}$ features a unique parent node ζ_b and a set C_b of children nodes. The active and reactive power balance equations for a node $b \in \mathcal{B}$ are given by the power flow model [37,38], as

$$P_{\zeta_b,s,t} = \sum_{c \in C_b} P_{bc,t,s} - r_{\zeta_b b} I_{\zeta_b b} - p_{b,s,t}, \quad \forall b \in \mathcal{B}, s \in S, t \in \mathcal{T}, \tag{12}$$

and

$$Q_{\zeta_b,s,t} = \sum_{c \in C_b} Q_{bc,t,s} - x_{\zeta_b b} I_{\zeta_b b} - q_{b,s,t},$$
$$\forall b \in \mathcal{B}, s \in S, t \in \mathcal{T}, \tag{13}$$

respectively, where $P_{\zeta_b,s,t}$ ($Q_{\zeta_b,s,t}$) is the active (reactive) power flowing in line (ζ_b, b), $I_{\zeta_b b}$ is the squared magnitude of the line's current, parameter $r_{\zeta_b b}$ ($x_{\zeta_b b}$) is the line's resistance (reactance), and $p_{b,s,t}$ ($q_{b,s,t}$) is the node's net power injection, which is defined by the node's wind generation $P_{b,s,t}^W$, storage charge–discharge decisions $P_{b,s,t}^{Ch}$ - $P_{b,s,t}^{Dc}$, power demand $D_{b,t}^P$ and demand-response actions (namely load shifting $P_{b,t}^{LS}$ and curtailment $P_{b,s,t}^{LC}$) thereupon, as well as by the power demand $P_{b,s,t}^{ERS}$ of the ERS. The formulation reads

$$p_{b,s,t} = D_{b,t}^P + P_{b,s,t}^{LS} - P_{b,s,t}^{LC} + P_{b,s,t}^{Ch} - P_{b,s,t}^{Dc} - P_{b,s,t}^W + P_{b,s,t}^{ERS}$$
$$\forall b \in \mathcal{B}, s \in S, t \in \mathcal{T}, \tag{14}$$

while the reactive power injection is defined in a similar manner as:

$$q_{b,s,t} = D_{b,t}^Q - Q_{b,t}^{CAP} - Q_{b,s,t}^W$$
$$\forall b \in \mathcal{B}, s \in S, t \in \mathcal{T}, \tag{15}$$

with $Q_{b,t}^{CAP}$ denoting the reactive power injection of the node's capacitor bank.

The voltage drop between ζ_b and b is given by

$$V_{\zeta_b,s,t} - 2 \left(R_{\zeta_b b} P_{\zeta_b b,t} + X_{\zeta_b b} Q_{\zeta_b b,t} \right) - \left(R_{\zeta_b b}^2 + X_{\zeta_b b}^2 \right) I_{\zeta_b b,t}$$
$$= V_{b,s,t}, \quad \forall b \in \mathcal{B}, n \in \mathcal{N}, t \in \mathcal{T}, \tag{16}$$

where $V_{b,s,t}$ is the node's voltage (squared magnitude). Branch power flows are calculated using the inequality

$$V_{b,s,t} I_{\zeta_b b,t} \geq P_{\zeta_b b,t}^2 + Q_{\zeta_b b,t}^2, \forall b \in \mathcal{B}, n \in \mathcal{N}, t \in \mathcal{T}, \tag{17}$$

as prescribed by the second-order conic relaxation model [39]. The safe operation of the APDN demands that all voltages remain within safe bounds:

$$\underline{V} \leq V_{b,s,t} \leq \overline{V} \quad \forall b \in \mathcal{B}, s \in S, t \in \mathcal{T}. \tag{18}$$

Finally, the electricity cost C_s^{APDN} of the APDN is given as

$$C_s^{APDN} = \sum_{t \in \mathcal{T}} P_{0,t,s} \pi_{s,t}^M + C_s^{DR} + C_s^{ESS}, \quad \forall s \in S, \tag{19}$$

and comprises the monetary cost of drawing active power $P_{0,t,s}$ from the main power system, at a price $\pi_{s,t}^M$, through the APDN's root node (numbered as node 0 by convention), as well as the costs C_s^{DR} and C_s^{ESS} induced by demand-response and storage charge–discharge actions (to be defined below).

2.2.1. Energy storage systems

The energy storage systems are deployed in APDN in order to enhance the flexibility of operation by managing the charging and discharging actions. The state of charge of the battery at node b is denoted by $E_{b,s,t}$, and follows the dynamics

$$E_{b,s,t} = E_{b,s,t-1} \cdot (1 - d_b) - \frac{1}{\eta_b^d} P_{b,s,t}^{Dc} + \eta_b^c P_{b,s,t}^{Ch},$$
$$\forall b \in \mathcal{B}, s \in S, t \in \mathcal{T}, \tag{20}$$

where d_b is a self-discharge parameter and η_b^c, η_b^d are charge–discharge efficiency parameters. The state of charge and charging/discharging power, are bounded as in

$$\underline{E}_b \leq E_{b,s,t} \leq \overline{E}_b, \quad \forall b \in \mathcal{B}, t \in \mathcal{T}. \tag{21}$$

$$P_{b,s,t}^{Ch} \leq \overline{P}_b^{Ch} \varrho_{b,s,t}, \quad \forall b \in \mathcal{B}, t \in \mathcal{T}, \tag{22}$$

$$P_{b,s,t}^{Dc} \leq \overline{P}_b^{Dc} (1 - \varrho_{b,s,t}), \quad \forall b \in \mathcal{B}, t \in \mathcal{T}, \tag{23}$$

The binary variable $\varrho_{b,s,t}$ prevents simultaneous charging and discharging. Finally, charging and discharging the battery brings a battery degradation cost modeled as

$$C_{b,s,t}^d = \frac{\frac{1}{\eta_b^d} P_{b,s,t}^{Dc} + \eta_n^c P_{b,s,t}^{Ch}}{2(\overline{E}_b - \underline{E}_b)} d_b, \quad \forall b \in \mathcal{B}, t \in \mathcal{T}. \tag{24}$$

Based on the above, the system's cost for charge–discharge actions is given by

$$C_s^{ESS} = \sum_{b \in \mathcal{B}} \sum_{t \in \mathcal{T}} C_{b,s,t}^d \tag{25}$$

2.2.2. Wind power modeling

A wind turbine's active and reactive generation is limited by respective upper and lower bounds, as in

$$0 \leq P_{b,s,t}^W \leq \hat{P}_{b,s,t}^W, \quad \forall b \in \mathcal{B}, s \in S, t \in \mathcal{T}, \tag{26}$$

$$Q_{b,s,t}^W \leq \sqrt{(S_{b,s,t}^W)^2 - (P_{b,s,t}^W)^2}, \forall b \in \mathcal{B}, s \in S, t \in \mathcal{T}. \tag{27}$$

where the (maximum) wind power output $\hat{P}_{b,s}^W$ is a scenario-dependent random variable.

2.3. Demand response flexibility

A flexible load can curtail or shift its energy consumption across time in response to pricing signals. A utility company, acting on behalf of the loads, decides whether to shift or curtail based on the received price signal from the APDN operator. For ease of presentation, we assume one load per each APDN node. In the formulations that follow, we denote each constraint's corresponding dual variable at the right of the constraint after a colon. The amount of energy that is shifted cannot exceed the energy that is curtailed, as in

$$\sum_{t \in \mathcal{T}} P_{b,s,t}^{LS} \leq \sum_{t \in \mathcal{T}} P_{b,s,t}^{LC}, \quad : \phi_{b,s}, \quad \forall b \in \mathcal{B}, s \in S. \tag{28}$$

The amount of energy that was demanded by a load/node, but was not supplied to it, is defined as

$$P_{b,s}^{NS} = \sum_{t \in \mathcal{T}} P_{b,s,t}^{LC} - \sum_{t \in \mathcal{T}} P_{b,s,t}^{LS}, \quad : \varphi_{b,s}, \quad \forall b \in \mathcal{B}, s \in S. \tag{29}$$

The total demand energy and power curtailment and shifts are a portion of the initial energy demands over the period, as in

$$\sum_{t \in \mathcal{T}} P_{b,s,t}^{LS} \leq \sum_{t \in \mathcal{T}} \Theta_b D_{b,t}^P \quad : \omega_{b,s} \tag{30}$$

$$\sum_{t \in \mathcal{T}} P_{b,s,t}^{LC} \leq \sum_{t \in \mathcal{T}} \Theta_b D_{b,t}^P \quad : \sigma_{b,s} \tag{31}$$

$$P_{b,s,t}^{LS} \leq \Gamma_b D_{b,t}^P \quad : \iota_{b,s,t} \tag{32}$$

$$P_{b,s,t}^{LC} \leq \Gamma_b D_{b,t}^P \quad : \varpi_{b,s,t} \tag{33}$$

$\forall b \in \mathcal{B}, s \in S.$

Each flexible load is controlled by the utility company with which it is registered. Each utility co-optimizes a portfolio of flexible loads, by determining the amount of energy that can be shifted or curtailed, with the purpose of minimizing its energy cost or maximizing its profit.
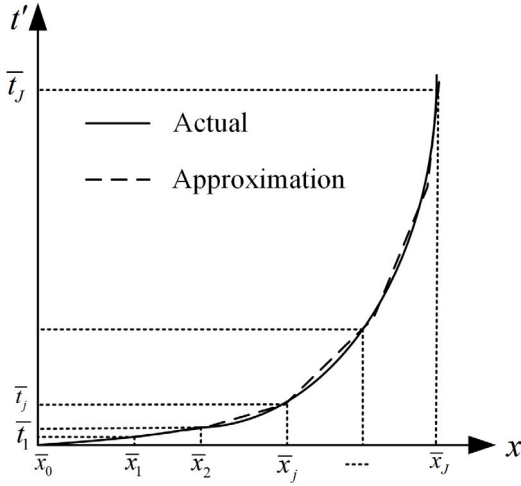
Fig. 2. Piecewise linear approximation of the BRP function.

This is driven by an incentive price $\pi_{g,t,s}^{\mathrm{AG}}$ for demand curtailment. Let $\mathbb{I}_{bg}$ indicate whether the load at APDN node b is registered with utility company $g \in \mathcal{G}$. A utility company's decision is formulated as the following cost-minimization problem:

$$
\begin{aligned}
C_{g,s}^{\mathrm{DR}} = \\
\min_{\Xi}\left\{ \sum_{t\in\mathcal{T}}\sum_{b\in B}\sum_{s\in S}\rho_s\mathbb{I}_{bg}\left(P_{b,s,t}^{\mathrm{LC}}\cdot(\mathrm{c}_{b,t}^{\mathrm{DR}}-\pi_{g,t,s}^{\mathrm{AG}})+\mathrm{c}_b^{\mathrm{LL}}P_{b,s}^{\mathrm{NS}}\right)\right\}
\end{aligned} \tag{34}
$$
$$
\text{s.t.} \quad (30)\text{–}(33), \quad \forall g \in \mathcal{G}.
$$

where Ξ represents the set of decision variables at the lower-level problem, including $P_{b,s,t}^{\mathrm{LC}}$, $P_{b,s,t}^{\mathrm{LS}}$, and $P_{b,s}^{\mathrm{NS}}$, and $\mathrm{c}_{b,t}^{\mathrm{DR}}, \mathrm{c}_b^{\mathrm{LL}}$ are cost parameters representing the compensation that the utility company needs to pay to the load users when curtailing or not serving them. Thus, the system's DR cost is given by

$$
C_s^{\mathrm{DR}} = \sum_{g\in\mathcal{G}}C_{g,s}^{\mathrm{DR}}, \quad \forall s \in S. \tag{35}
$$

We have now defined all the elements of the coupled system's optimization problem (2). Notably, the DR cost of the system is governed by a set of (lower-level) optimization problems (one for each utility company) and the operator can only affect it indirectly, by deciding on the incentive prices $\pi_{g,t,s}^{\mathrm{AG}}$.

3. Solution methodology

In this section, we present the methodology of solving problem (2). Attributing to the uncertainty of the problem's random variables (traffic demand and wind generation), the EV drivers' selfish routing choices, and the utility companies' deliberate DR actions, problem (2) takes the form of a cost-minimizing stochastic Wardrop-Stackelberg equilibrium problem. The problem is non-convex and bi-level. In what follows, we present (one by one) the techniques used to bring the problem in a form that standard solvers can handle.

3.1. Linearization and convexification of ERS model

There are four non-linearities in the problem formulation including (3), (4), (9) and (11).

Let us begin with Eq. (4). We deploy a piecewise linear approximation to linearize (4) in (36)–(45). Specifically, we replace the nonlinear term $x_{a,s,t}^4$ with $\bar{t}_j$. Then, $\bar{t}_j$ is approximated through a set of linear functions, as shown in Fig. 2. Let U^l, L^l and N^l denote the upper limit,

lower limit, and number of the approximated segments, respectively. Then, the slope of each segment is obtained in (36)–(39). Eq. (40) indicates the mathematical linear equation form. The binary variable $U_{a,s,t,j}^x$ in the equation guarantees that the equation is implemented if and only if a segment is selected. Eqs. (41)–(42) declares that the value of the traffic demands in each segment should respect the upper and lower bounds of the segment. The approximated traffic flow is recast in (43) to be used in the problem dropping index j. Based on (44), only one segment should be selected. $t_{a,s,t,j}^l$ is valid if a segment selected in (45), and its value is calculated in (46).

$$
\Delta x = \frac{U^l - L^l}{N^l} \tag{36}
$$

$$
\bar{x}_j = L^l + (j-1)\Delta x \tag{37}
$$

$$
\Delta t_j = \bar{x}_{j+1}^4 - \bar{x}_j^4 \tag{38}
$$

$$
m_j^{slope} = \frac{\Delta t_j}{\Delta x} \tag{39}
$$

$$
t_{a,s,t,j}^l = m_j^{slope}\cdot(x_{a,s,t,j}^l - \bar{x}_j U_{a,s,t,j}^x) + \bar{t}_j U_{a,s,t,j}^x \tag{40}
$$

$$
x_{a,s,t,j}^l \geq \bar{x}_j\cdot U_{a,s,t,j}^x \quad \forall j\in\mathcal{J}, t\in\mathcal{T}, a\in\mathcal{A}, s\in S \tag{41}
$$

$$
x_{a,s,t,j}^l \leq \bar{x}_{j+1}\cdot U_{a,s,t,j}^x \quad \forall j\in\mathcal{J}, t\in\mathcal{T}, a\in\mathcal{A}, s\in S \tag{42}
$$

$$
x_{a,s,t} = \sum_{j\in\mathcal{J}}x_{a,s,t,j}^l \quad \forall t\in\mathcal{T}, a\in\mathcal{A}, s\in S \tag{43}
$$

$$
\sum_{j\in\mathcal{J}}U_{a,s,t,j}^x = 1 \quad \forall t\in\mathcal{T}, a\in\mathcal{A}, s\in S \tag{44}
$$

$$
t_{a,s,t,j}^l \leq M\cdot U_{a,s,t,j}^x \quad \forall j\in\mathcal{J}, t\in\mathcal{T}, a\in\mathcal{A}, s\in S \tag{45}
$$

$$
t_{a,s,t}' = \sum_{j\in\mathcal{J}}t_{a,s,t,j}^l \quad \forall j\in\mathcal{J}, t\in\mathcal{T}, a\in\mathcal{A}, s\in S \tag{46}
$$

In order to linearize (9), we apply the McCromick convexification method [40]. To do so, the auxiliary variable $Y_{g,d,s,t}^{\mathrm{AUX}}$ is replaced with the nonlinear part. Then, the following mathematical formulation is developed as

$$
\begin{aligned}
Y_{g,d,s,t}^{\mathrm{AUX}} &\geq f_{k,s,t}\tau^{\min} + f^{\min}\tau_{k,s,t} - \tau^{\min}f^{\min} \\
Y_{g,d,s,t}^{\mathrm{AUX}} &\geq f_{k,s,t}\tau^{\max} + f^{\max}\tau_{k,s,t} - \tau^{\max}f^{\max} \\
Y_{g,d,s,t}^{\mathrm{AUX}} &\leq f_{k,s,t}\tau^{\min} + f^{\max}\tau_{k,s,t} - \tau^{\max}f^{\min} \\
Y_{g,d,s,t}^{\mathrm{AUX}} &\leq f_{k,s,t}\tau^{\max} + f^{\min}\tau_{k,s,t} - \tau^{\min}f^{\max}
\end{aligned} \tag{47}
$$

The objective function (Eq. (3)) of the ERS can be written via the equivalent transformation as [23]:

$$
\begin{aligned}
\sum_{a\in\mathcal{A}}\sum_{t\in\mathcal{T}}\sum_{s\in S}\rho_s\left[(\omega\tau_{a,s,t}+T_a^C)x_{a,s,t}\right] = \\
\sum_{a\in\mathcal{A}}\sum_{t\in\mathcal{T}}\sum_{d\in D}\sum_{k\in\mathcal{K}}\sum_{s\in S}\rho_s\left[(\omega\tau_{a,s,t}+T_a^C)f_{k,s,t}\delta_{a,s,k}^d\right] = \\
\sum_{t\in\mathcal{T}}\sum_{s\in S}\sum_{d\in D}\sum_{k\in\mathcal{K}}\rho_s\left[c_{k,s,t}f_{k,s,t}\right] = \\
\sum_{t\in\mathcal{T}}\sum_{s\in S}\rho_s\left[\sum_{d\in D}u_{d,s,t}\sum_{k\in\mathcal{K}}f_{k,s,t}\right] = \\
\sum_{t\in\mathcal{T}}\sum_{s\in S}\rho_s\left[\sum_{d\in D}u_{d,s,t}F_{s,t}^d\right]
\end{aligned} \tag{48}
$$

where the expression in (48) is bilinear for the proposed framework, but can again be convexified using the McCromick method. Moreover, for the static solution used later on to compare the results, the expression becomes linear.

Finally, the well-known big-M method presented in [41] is utilized to linearize (11) as

$$
f_{k,s,t} \leq I_{k,s,t}M \tag{49}
$$

$$\tau_{k,s,t} - u_{d,s,t} \leq (1 - I_{k,s,t})M \tag{50}$$

$$f_{k,s,t}, (c_{k,s,t} - u_{d,s,t}) \geq 0 \tag{51}$$

The approximation techniques presented for Eqs. (3), (4), (9) can result in optimality gaps in general. However, it is well known that the McCormick relaxations can be made progressively tighter by using piecewise-linear approximations of the expression's bounds instead of simple linear ones. In turn, the accuracy of the piece-wise linear approximations can be enhanced by augmenting the number of segments (at the expense of higher computational time due to introducing more variables). Thereby, one can choose the trade-off between the optimality gap for the proposed method and the computational time. Nevertheless, for the stochastic program presented, it is not the accuracy of the piecewise linear approximations, but the number of scenarios that dominates the efficiency-complexity trade-off in practice and, thus, tightening the relaxations is not motivated for this paper's problem.

3.2. APDN upper-level problem

We assume that the coupled transport and distribution problem is managed by a non-profit system operator in order to minimize the social cost stemming from the objectives of the ERS and APDN. The coupled objective function is at the upper-level problem as

$$\min \quad \sum_{t \in \mathcal{T}} \sum_{s \in S} \sum_{b \in B} \rho_s \left(\sum_{d \in D} u_{d,s,t} F_{s,t}^d + \pi_{t,s}^{\mathrm{M}} P_{b,s,t}^{\mathrm{M}} \right.$$
$$\left. + \sum_{g \in \mathcal{G}} \pi_{g,t,s}^{\mathrm{AG}} P_{b,s,t}^{\mathrm{LC}} + C_{b,s,t}^{\mathrm{d}} \right) \tag{52}$$

where the first term is the objective of ERS coming from (48). The second term indicates electricity purchased from the electricity market. The third term shows the cost of load shifting in the interaction with the set of utility companies, and the last term indicates the energy storage system cost.

3.3. Utility company lower-level problem

The proposed framework for the set of utility companies in 2.3 is at the lower level. The KKT conditions are used to transfer the lower-level problem to the upper-level [41]. The derived equations are given in (53) to (60).

$$c_{b,t}^{\mathrm{DR}} - \varphi_{g,b,s} + \sigma_{g,b,s} + \varpi_{g,b,s,t} - \phi_{g,b,s} - \pi_{g,t,s}^{\mathrm{AG}} = 0 \tag{53}$$

$$\varphi_{g,b,s} + c_b^{\mathrm{LL}} = 0 \tag{54}$$

$$\phi_{g,b,s} + \varphi_{g,b,s} + \omega_{g,b,s} + \iota_{g,b,s,t} = 0 \tag{55}$$

$$\omega_{g,b,s}\left(\sum_{t \in \mathcal{T}} P_{b,s,t}^{\mathrm{LS}} - \sum_{t \in \mathcal{T}} \Theta_b D_{b,t}^{\mathrm{P}}\right) = 0, \quad \forall g \in \mathcal{G}, b \in \mathcal{Z}_g, s \in S, \tag{56}$$

$$\sigma_{g,b,s}\left(\sum_{t \in \mathcal{T}} P_{b,s,t}^{\mathrm{LC}} - \sum_{t \in \mathcal{T}} \Theta_b D_{b,t}^{\mathrm{P}}\right) = 0, \quad \forall g \in \mathcal{G}, b \in \mathcal{Z}_g, s \in S, \tag{57}$$

$$\phi_{g,b,s}\left(\sum_{t \in \mathcal{T}^D} P_{b,s,t}^{\mathrm{LS}} - \sum_{t \in \mathcal{T}^I} P_{b,s,t}^{\mathrm{LC}}\right) = 0, \quad \forall g \in \mathcal{G}, b \in \mathcal{Z}_g, s \in S, \tag{58}$$

$$\iota_{g,b,s,t}(P_{b,s,t}^{\mathrm{LS}} - \Gamma_b D_{b,t}^{\mathrm{P}}) = 0, \quad \forall g \in \mathcal{G}, b \in \mathcal{Z}_g, s \in S, \tag{59}$$

$$\varpi_{g,b,s,t}(P_{b,s,t}^{\mathrm{LC}} - \Gamma_b D_{b,t}^{\mathrm{P}}) = 0, \quad \forall g \in \mathcal{G}, b \in \mathcal{Z}_g, s \in S, \tag{60}$$

The term $\pi_{g,t,s}^{\mathrm{AG}} P_{b,s,t}^{\mathrm{LC}}$ in (34) is a bilinear product. The strong duality theorem is applied to linearize the bilinear product, and the result is as follows.

$$G^{g,t,s} = -\sum_{b \in \mathcal{Z}_g} \left(\sigma_{g,b,s} \Theta_b D_{b,t}^{\mathrm{P}} + \omega_{g,b,s} \Theta_b D_{b,t}^{\mathrm{P}} + \iota_{g,b,s,t} \Gamma_b D_{b,t}^{\mathrm{P}} \right.$$
$$\left. + \varpi_{g,b,s,t} \Gamma_b D_{b,t}^{\mathrm{P}} \right) + c_{b,t}^{\mathrm{DR}} P_{b,s,t}^{\mathrm{LC}} + c_b^{\mathrm{LL}} P_{b,s}^{\mathrm{NS}}, \tag{61}$$
$$\forall g \in \mathcal{G}, s \in S, t \in \mathcal{T}.$$

In (53) to (57), $\omega_{g,b,s}$, $\sigma_{g,b,s}$, $\phi_{g,b,s}$, $\varpi_{g,b,s,t}$ and $\iota_{g,b,s,t}$ are non-negative. The nonlinear complementary slackness conditions (56)–(60) are equivalently represented as a set of linear equations using big-M method as presented in 3.1.

$$\omega_{g,b,s} \leq M_1 u_{g,b,s}, \quad \forall g \in \mathcal{G}, b \in \mathcal{Z}_g, s \in S, \tag{62}$$

$$\sum_{t \in \mathcal{T}} P_{b,s,t}^{\mathrm{LS}} - \sum_{t \in \mathcal{T}} \Theta_b D_{b,t}^{\mathrm{P}} \leq M_2(1 - u_{g,b,s}),$$
$$\forall g \in \mathcal{G}, b \in \mathcal{Z}_g, s \in S, \tag{63}$$

$$\sigma_{g,b,s} \leq M_1 o_{g,b,s}, \quad \forall g \in \mathcal{G}, b \in \mathcal{Z}_g, s \in S, \tag{64}$$

$$\sum_{t \in \mathcal{T}} P_{b,s,t}^{\mathrm{LC}} - \sum_{t \in \mathcal{T}} \Theta_b D_{b,t}^{\mathrm{P}} \leq M_2(1 - o_{g,b,s}),$$
$$\forall g \in \mathcal{G}, b \in \mathcal{Z}_g, s \in S, \tag{65}$$

$$\phi_{g,b,s} \leq M_1 h_{g,b,s}, \quad \forall g \in \mathcal{G}, b \in \mathcal{Z}_g, \tag{66}$$

$$\sum_{t \in \mathcal{T}^D} P_{b,s,t}^{\mathrm{LS}} - \sum_{t \in \mathcal{T}^I} P_{b,s,t}^{\mathrm{LC}} \leq M_2(1 - h_{g,b,s}),$$
$$\forall g \in \mathcal{G}, b \in \mathcal{Z}_g, s \in S, \tag{67}$$

$$\iota_{g,b,s,t} \leq M_1 r_{g,b,s,t}, \quad \forall g \in \mathcal{G}, b \in \mathcal{Z}_g, s \in S, \tag{68}$$

$$P_{b,s,t}^{\mathrm{LS}} - \Gamma_b D_{b,t}^{\mathrm{P}} \leq M_2(1 - r_{g,b,s,t}),$$
$$\forall g \in \mathcal{G}, b \in \mathcal{Z}_g, s \in S, \tag{69}$$

$$\varpi_{g,b,s,t} \leq M_1 y_{g,b,s,t}, \quad \forall g \in \mathcal{G}, b \in \mathcal{Z}_g, s \in S, \tag{70}$$

$$P_{b,s,t}^{\mathrm{LC}} - \Gamma_b D_{b,t}^{\mathrm{P}} \leq M_2(1 - y_{g,b,s,t}),$$
$$\forall g \in \mathcal{G}, b \in \mathcal{Z}_g, s \in S, \tag{71}$$

Finally, the upper-level objective function is modified, transferring the lower-level objective function subject to (5)–(8), (12)–(18), (20)–(34), (36)–(51), (53)–(55), (61), and (62)–(71).

$$\min \quad \sum_{t \in \mathcal{T}} \sum_{s \in S} \sum_{b \in B} \rho_s \left(\sum_{d \in D} u_{d,s,t} F_{s,t}^d + \pi_{t,s}^{\mathrm{M}} P_{b,s,t}^{\mathrm{M}} + \sum_{g \in \mathcal{G}} G^{g,t,s} \right.$$
$$\left. + C_{b,s,t}^{\mathrm{d}} + PF \cdot V_{b,s,t}^{\mathrm{DEV}} \right) \tag{72}$$

$$V_{b,s,t} \geq \underline{V} - V_{b,s,t}^{\mathrm{DEV}} \tag{73}$$

Due to the feasibility concerns, we disregard the minimum voltage bound, and we use a penalty term in (72) and add a new constraint as in (73).

4. Numerical experiments and results

In this section, we introduce the coupled ERS and APDN system used as an evaluation setup, and then we present the simulation results. We investigate the effect of the ERS on the APDN with and without the integration of flexibility in APDN. We aim to demonstrate the effect of flexibility potential in the coupled problem. Besides, we exhibit the effect of uncertainties on the distribution of traffic demands on the roads.

4.1. Case study

The proposed approach has been tested on 12-node ERS and 33-node APDN toward demonstrating the effectiveness of the proposed framework. The data of the ERS and APDN are adopted from [4] and [33], respectively. The parameters of the roads are provided in Table 2. The ERS links are electrified by the APDN as shown in Fig. 3, where the electrified links are determined by the nodes e.g. B_2, B_4, etc. The roads are bidirectional from $a_1 - a_{40}$. However, for the sake of brevity, we only show $a_1 - a_{20}$, and the reverse road link number can be obtained by adding 20 to the paired link. For instance, the

Table 2
Parameters of road links.

Link	c_a(p.u.)	τ_a^0(min)	Link	c_a(p.u.)	τ_a^0(min)
a_1	18	6	a_{11}	13.8	12.5
a_2	9.8	5	a_{12}	20	10.5
a_3	20	10	a_{13}	8.9	5.8
a_4	7.9	5.5	a_{14}	13.2	11
a_5	17	6.5	a_{15}	9.15	5.9
a_6	8.5	6	a_{16}	17.5	6.3
a_7	13.5	12	a_{17}	9.76	5.7
a_8	8.2	6.5	a_{18}	8.97	5.8
a_9	19	10.2	a_{19}	18.2	6.1
a_{10}	14	11.5	a_{20}	20	9.8

Table 3
O-D pairs and according traffic demands (pu)

O-D pair	Scenario			
	#1	#2	#3	#4
T1-T6	15	13	17	12
T3-T6	25	23	26	22
T1-T12	10	11	10	9
T1-T10	15	16	15	17
T1-T11	15	15	16	16
T4-T12	15	14	16	15
T3-T10	20	18	23	21
T3-T12	12	11	14	12
T4-T11	5	2	4	3
T4-T9	10	10	7	9
T4-T10	8	7	7	6

pair of a_1 is a_{21}. There are 11 O-D pairs, and four scenarios are generated for each, using the normal distribution function. The mean value of the pairs are obtained from [4], and the generated scenarios are given in Table 3. The monetary cost is also assumed to be 10 $/h. There are three types of consumers, including residential (nodes 1–22), commercial (nodes 23–25), and industrial (nodes 26–33). Each type of usage is called a zone, and each zone is served through a utility company. There is a battery storage system at node 17 with a maximum charging/discharging capacity of 50 kW/h, and an efficiency of 0.95. The total capacity of the BES, the number of life cycles, and the total capital cost of the battery storage system are 100 kW, 10000, and 15000 $, respectively. Fig. 4 shows the pattern of the electrical demands that have been driven from [42,43], traffic demands [4], expected wind power generation [44], and expected electricity market prices [45]. The uncertainty of the electricity market prices and wind power generation are addressed via four scenarios incorporating a 15% and 20% deviation for electricity and wind power generations using a normal distribution function. Given the consideration of four scenarios for each source of uncertainty, the resultant combination yields a total of 64 scenarios. Then, in order to enhance computational efficiency and maintain tractability, the number of scenarios is reduced to ten. The scenario reduction is conducted by deploying the Kantorovich probability distance presented in [46]. It is also assumed that a maximum of 15% of the energy of each consumer can be reduced, while the amount of power curtailed at each hour cannot exceed 30%. The electricity not supplied costs 100$/MWh, 300$/MWh, and 300$/MWh for consumers types one, two and three, respectively. There are five wind turbines with a similar generation capacity of 100 kW, located in nodes 16, 18, 22, 28, and 33. Finally, the minimum and maximum voltage magnitudes are 0.9 and 1.1 pu, respectively.

4.2. Results and discussion

Fig. 5 exhibits the results of traffic flows at traffic rush hour at hour 19 (19:00) on the existing links in two sample scenarios #1 and #7, where the value of scenario #3 in Table 3 is represented here as scenario #7 after combination with other uncertainty sources. It can

(a) ERS perspective

(b) APDN perspective
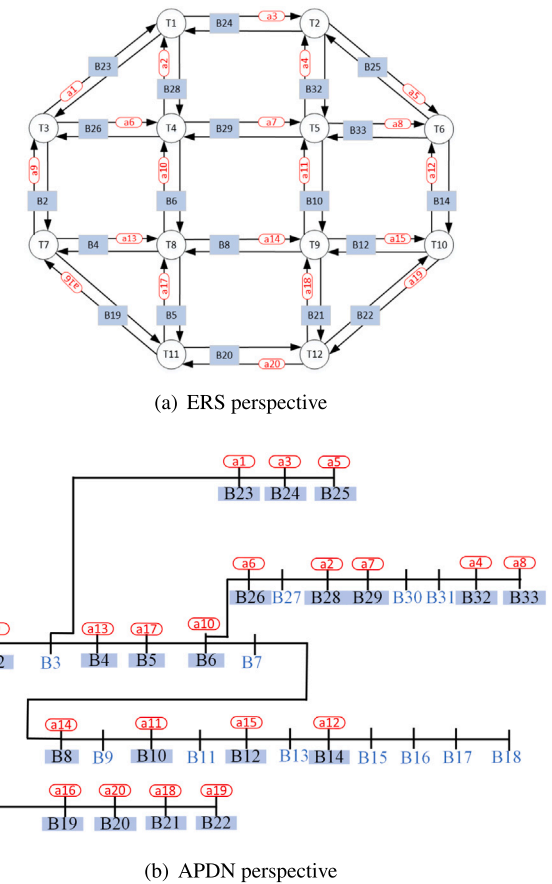
Fig. 3. Coupled 20 nodes ERS and 33-node APDN.
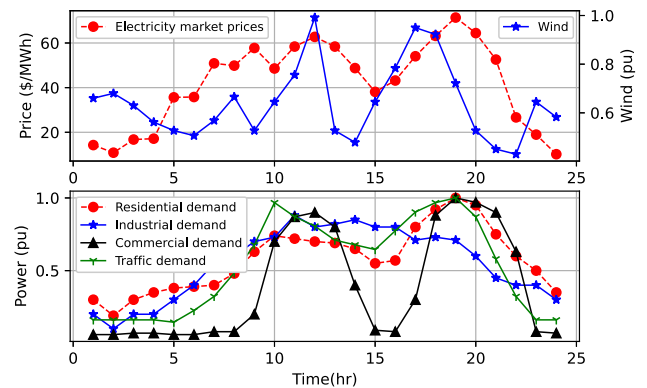
Fig. 4. Demands, electricity market prices, and wind power generation.

be seen that most drivers tend to travel on the outermost roads, which have the highest capacity and less travel time. Since the traffic demands of O–D pairs are different in the mentioned scenarios, the traffic flow distribution gives different values according to the demands. If (6), (8)–(9) are neglected in the traffic assignment problem, the proposed model turns into a static model. The results of the semi-dynamic model are also compared with the static solution in Fig. 5. An example clarifies the difference in the results. In the static form, without considering the congestion and the consequence residual time, the destinations of O–D pairs 3, 6, and 8 are node T12. Therefore, 37 pu should arrive at T12 in the scenario #1 overall. It can be seen that 37 arrives at T12 in static form while in dynamic solution, 36.11 arrives at T12 at hour 19 due to the existing congestion. Fig. 6 demonstrates the expected values
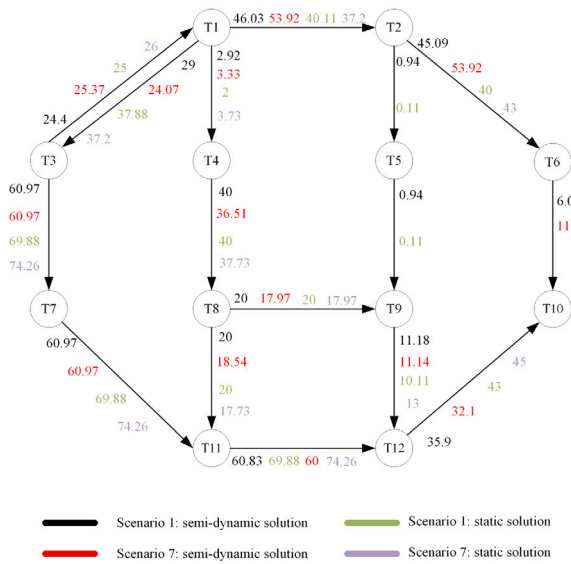
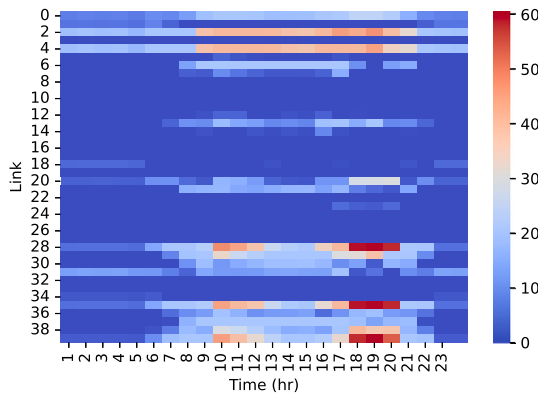**Fig. 5.** Comparing traffic flow results in two sample scenarios with static and dynamic solutions.

Fig. 6. Heat map showing the level of congestion on links.

Fig. 7. Average values of travel time on road segments.

Fig. 8. Results of the total DR compared to the input electrical demand.

Fig. 9. Expected electricity procurement by the electricity market and wind turbines.

of the link's traffic with respect to time and the links. The proposed heat map indicates the highest traffic during hours 18–20, which is in accordance with the transportation system rush hours, on links 29, 36, and 40. Fig. 7 depicts the average travel time across all scenarios and temporal periods for various links. It verifies the higher spent travel time on links 29, 30, and 40, as shown before in Fig. 6. Conversely, some other links, such as link 4, are not chosen by EV users, and only free-flow travel time is reported.

Fig. 8 depicts the results of activating the DR service in each zone. The maximum curtailment is carried out during hours 18–20 in accordance with the maximum electricity prices provided in Fig. 4. By considering the electricity prices, it can be seen from the figure that the DR services are activated during peak hours in order to reduce total electricity procurement costs. The curtailed electricity is shifted to the off-peak hours, which are more tolerable by the APDN. Fig. 9 shows the procured electricity from the electricity market to support the existing demands, including APDN and ERS demands. The amount of purchase from the electricity market fully respects the demands and price patterns given in Fig. 4. The maximum expected electricity is purchased in hour 19, which is equivalent to the maximum demand after the DR program plus the traffic demands. It is worth mentioning that the amount of electricity not supplied during the activation of DR is zero. That is, all curtailed electricity during peak hours is shifted to the off-peak hours. The utility company earns 202.4 $ by activating the DR program.
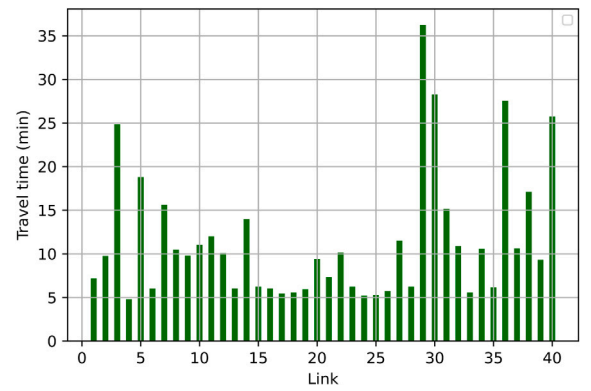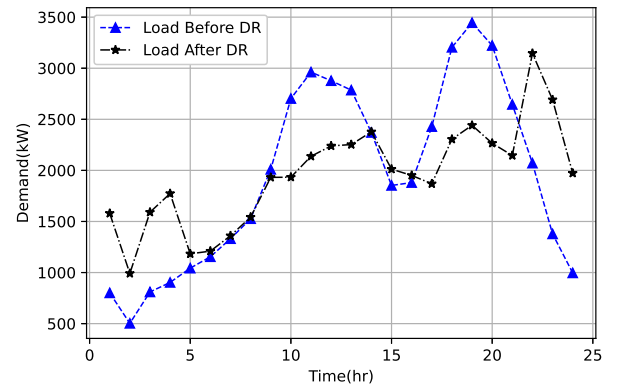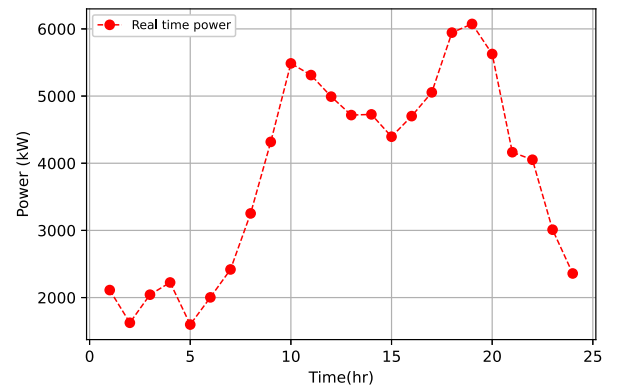
Fig. 10 depicts the charging, discharging, and state of charge of the battery energy storage. The energy arbitrage has been carried out properly based on the figure. The battery energy storage is discharged during the peak hours and charged during the off-peak hours in order to harvest the benefit of the difference between the peak and off-peak electricity prices. The state of charge in the battery energy storage yields the right behavior after each charging or discharging by increasing or decreasing.

Fig. 11 depicts the balance of energy procured and consumed in each hour, such that the positive values declare the demands and the negative values exhibit the supply. As evident, the electricity market at upstream of APDN is the main source of electricity procurement for two main demands of electrical and ERS charging. Compared to the electrical demands, the ERS demands are significant, specifically during its rush hours. Wind turbine generation is the second source of
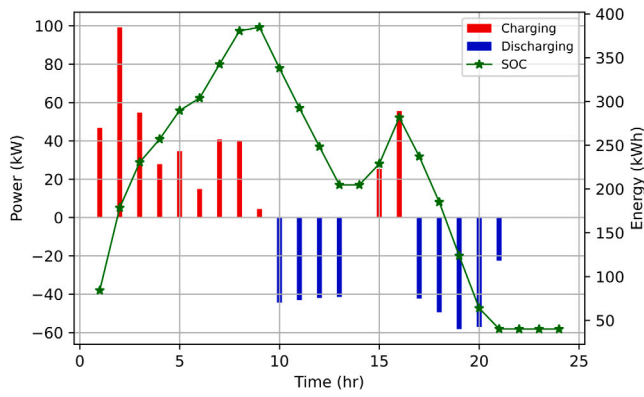
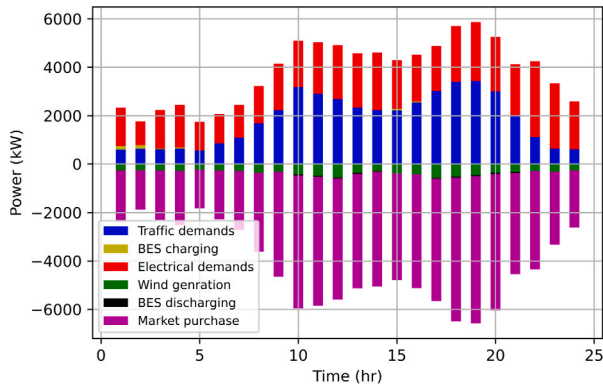**Fig. 10.** Expected charging/discharging scheduling of ESSs.

Fig. 11. Balance of generated and consumed electricity in both transportation and APDN.

Fig. 12. Output voltage with respect to the time and nodes.

Fig. 13. Effect of DR on lifting minimum voltage level.

Fig. 14. Effect of penetration of wind generation on total cost APDN and voltage.

procuring electricity. As a local generation, it can help supply demands locally and provide a safe operation. The battery energy system has been shown in both the supply and demand sides. When the battery is charged, it is treated as a load, while it is like a generator when it is discharged. Although the amount of charge/discharge does not show a remarkable value compared to the other sources, it is valuable in its node of location, and its performance is significant compared to the demand (generation) of the located APDN node ($B17$). It should be noted that the amount of demands in $B17$ is 60 kW while the amount of allowable charge/discharge is 150 kW.

Fig. 12 shows that even with using demand response and local wind generation, there are still violations in meeting the lower bound of the voltage (0.9 pu) that verifies the massive demands of the transportation systems. In order to reveal the effectiveness of the DR services in reducing the transportation network demands, Fig. 13 compares the minimum obtained voltage with and without activating the DR flexibility. It can be seen from the figure during the electricity demands peak hours, which overlapped with the transportation rush hours, the DR service has helped the system to enhance the voltage magnitude. It is worth mentioning that since the main technical challenge of the APDN in this problem is the violation of the lower limit of the voltage due to the massive ERS charging demands, the figure of the maximum bound is not depicted. However, it can be seen from Fig. 12 that the upper limit is satisfied in all APDN nodes during the whole time horizon. It is noteworthy that the lower limit of the voltage is mathematically possible to be violated. This is attributed to the formulation of the lower bound of voltage in Eq. (18), wherein its enforcement is primarily governed by a penalty term, per Eqs. (72) and (73).

Fig. 14 illustrates the impact of wind power generation on both the total cost and the voltage of APDN. The generation of wind turbines
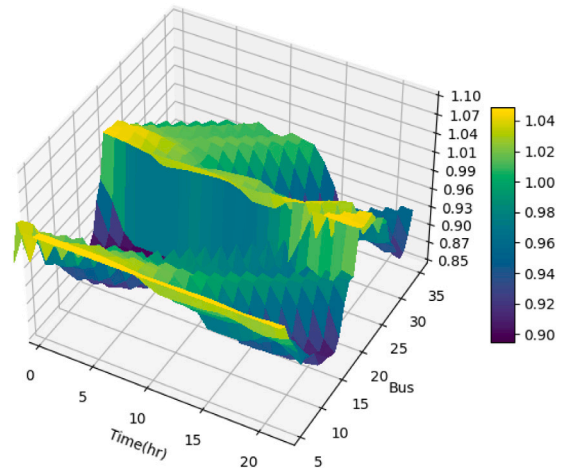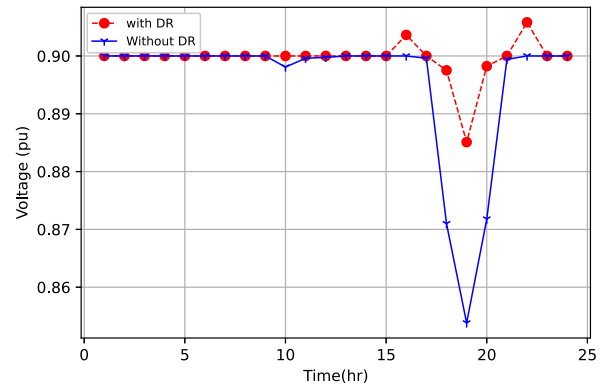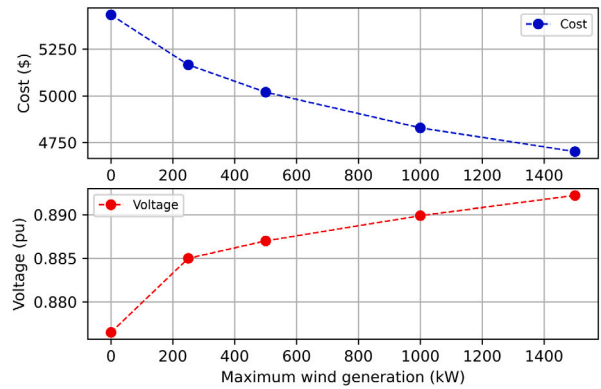
ranges from 0 to 1500 kW, and the results are recorded. The results reveal that the total cost decreases from 5434\$ to 4702\$ by an increase in the generation of wind turbines. It should be noted that maximum wind generation only indicates the total capacity, whereas actual generation naturally fluctuates across different time periods. As mentioned in the case study, existing turbines are located at APDN nodes 16, 18, 22, 28, and 33. That is, wind turbines perform as local generators to support parts of demands, which results in partly mitigating voltage drop. The higher the wind turbine's local generations, the lower the voltage drop.

5. Conclusion

This study has proposed a framework to solve the coupled problem of ERS and APDN with high penetration of local wind turbine uncertainty using a stochastic programming approach by integrating the flexibility of demand response service and battery energy storage. The objective is to minimize the total cost of APDN and the imposed travel time to ERS. The following items declare the conclusion of the paper point-by-point.

- Simulation results yield the APDN dispatch actions concerning the resources of each APDN, purchases from the electricity market, responses of the DR providers (i.e. utility company) at the lower level, as well as the decisions related to traffic flow distribution in the ERS.
- The traffic flow distributions pursue their uncertain demands and give optimal solutions based on the capacity of the links.
- The dynamic nature of the problem affects the number of EVs arriving at each destination due to the residual time of travel coming from traffic congestion.
- The DR program shows curtailment and shifting the load based on the electricity price signals. The implemented DR can significantly facilitate the operation of APDN coordinated with ERS to lift up the minimum obtained voltage by 3.66% and keep the APDN operation safe.

Even though this paper has enriched the literature on coupled electrified road systems and active power distribution networks integrated by demand response, it is imperative to acknowledge that several avenues for future research and unresolved challenges persist within this domain. First, one of the primary solutions to support the charging demands of EVs on ERS is to improve the infrastructure in APDN. Hence, a renewable energy source hosting capacity can be an approach to hosting the required generation at APDN, respecting cleaner production and sustainable energy alongside the meeting charging demands of EVs. Second, the time frame of one-hour resolution gives a semi-dynamic approach that is used in the current study. However, using a more nuanced time resolution is still challenging for researchers due to the complex aspects of dynamic user equilibrium. It will be challenging but interesting to use a well-established dynamic traffic assignment problem in our proposed analysis framework, promising a more comprehensive analysis. Third, in this paper we have addressed only selfish drivers, assuming rational EV users. However, in reality, some EV users may exhibit different behaviors. In addition, we consider that EV users have perfect information about the routes, while, in reality, not all EV users have perfect information.

CRediT authorship contribution statement

Arsalan Najafi: Conceptualization, Data curation, Formal analysis, Investigation, Methodology, Resources, Software, Validation, Visualization, Writing – original draft, Writing – review & editing. **Georgios Tsaousoglou:** Writing – review & editing, Methodology, Investigation, Conceptualization, Formal analysis. **Kun Gao:** Writing – review & editing, Validation, Resources, Project administration, Investigation, Funding acquisition, Formal analysis, Conceptualization. **Omkar Parishwad:** Investigation, Methodology, Visualization, Writing – review & editing.

Declaration of competing interest

The authors declare that they have no known competing financial interests or personal relationships that could have appeared to influence the work reported in this paper.

Data availability

Data will be made available on request.

References

[1] Outlook GE. Global EV Outlook. 2023, Available online: https://www.iea.org/reports/global-ev-outlook-2023.

[2] Chen F, Taylor N, Kringos N. Electrification of roads: Opportunities and challenges. Appl Energy 2015;150:109–19. http://dx.doi.org/10.1016/j.apenergy.2015.03.067, URL https://www.sciencedirect.com/science/article/pii/S0306261915003591.

[3] Gutierrez-Alcoba A, Rossi R, Martin-Barragan B, Embley T. The stochastic inventory routing problem on electric roads. European J Oper Res 2023;310(1):156–67. http://dx.doi.org/10.1016/j.ejor.2023.02.024, URL https://www.sciencedirect.com/science/article/pii/S0377221723001601.

[4] Wei W, Wang J. Electrified transportation network. In: Modeling and optimization of interdependent energy infrastructures. Cham: Springer International Publishing; 2020, p. 343–454. http://dx.doi.org/10.1007/978-3-030-25958-7_5.

[5] Mubarak M, Üster H, Abdelghany K, Khodayar M. Strategic network design and analysis for in-motion wireless charging of electric vehicles. Transp Res E 2021;145:102179. http://dx.doi.org/10.1016/j.tre.2020.102179, URL https://www.sciencedirect.com/science/article/pii/S136655452030822X.

[6] Li S, Mi CC. Wireless power transfer for electric vehicle applications. IEEE J Emerg Sel Top Power Electron 2015;3(1):4–17. http://dx.doi.org/10.1109/JESTPE.2014.2319453.

[7] Chen Z, He F, Yin Y. Optimal deployment of charging lanes for electric vehicles in transportation networks. Transp Res B 2016;91:344–65. http://dx.doi.org/10.1016/j.trb.2016.05.018, URL https://www.sciencedirect.com/science/article/pii/S0191261516303319.

[8] Liu H, Zou Y, Chen Y, Long J. Optimal locations and electricity prices for dynamic wireless charging links of electric vehicles for sustainable transportation. Transp Res E 2021;152:102187. http://dx.doi.org/10.1016/j.tre.2020.102187, URL https://www.sciencedirect.com/science/article/pii/S1366554520308292.

[9] Ngo H, Kumar A, Mishra S. Optimal positioning of dynamic wireless charging infrastructure in a road network for battery electric vehicles. Transp Res D 2020;85:102385. http://dx.doi.org/10.1016/j.trd.2020.102385, URL https://www.sciencedirect.com/science/article/pii/S1361920920305721.

[10] Liu Z, Song Z. Robust planning of dynamic wireless charging infrastructure for battery electric buses. Transp Res C 2017;83:77–103. http://dx.doi.org/10.1016/j.trc.2017.07.013, URL https://www.sciencedirect.com/science/article/pii/S0968090X17301985.

[11] He J, Yang H, Huang H-J, Tang T-Q. Impacts of wireless charging lanes on travel time and energy consumption in a two-lane road system. Phys A 2018;500:1–10. http://dx.doi.org/10.1016/j.physa.2018.02.074, URL https://www.sciencedirect.com/science/article/pii/S037843711830150X.

[12] Shao C, Li K, Qian T, Shahidehpour M, Wang X. Generalized user equilibrium for coordination of coupled power-transportation network. IEEE Trans Smart Grid 2023;14(3):2140–51. http://dx.doi.org/10.1109/TSG.2022.3206511.

[13] Shao C, Li K, Hu Z, Shahidehpour M. Coordinated planning of electric power and natural gas distribution systems with refueling stations for alternative fuel vehicles in transportation system. IEEE Trans Smart Grid 2022;13(5):3558–69. http://dx.doi.org/10.1109/TSG.2022.3166965.

[14] Xie S, Hu Z, Wang J, Chen Y. The optimal planning of smart multi-energy systems incorporating transportation, natural gas and active distribution networks. Appl Energy 2020;269:115006. http://dx.doi.org/10.1016/j.apenergy.2020.115006, URL https://www.sciencedirect.com/science/article/pii/S0306261920305183.

[15] Xie S, Wu Q, Hatziargyriou ND, Zhang M, Zhang Y, Xu Y. Collaborative pricing in a power-transportation coupled network: A variational inequality approach. IEEE Trans Power Syst 2023;38(1):783–95. http://dx.doi.org/10.1109/TPWRS.2022.3162861.

[16] Xie S, Hu Z, Wang J. Two-stage robust optimization for expansion planning of active distribution systems coupled with urban transportation networks. Appl Energy 2020;261:114412. http://dx.doi.org/10.1016/j.apenergy.2019.114412, URL https://www.sciencedirect.com/science/article/pii/S0306261919320999.

[17] Qiao W, Han Y, Zhao Q, Si F, Wang J. A distributed coordination method for coupled traffic-power network equilibrium incorporating behavioral theory. IEEE Trans Veh Technol 2022;71(12):12588–601. http://dx.doi.org/10.1109/TVT.2022.3206095.

[18] Li J, Xu X, Yan Z, Wang H, Shahidehpour M, Chen Y. Coordinated optimization of emergency response resources in transportation-power distribution networks under extreme events. IEEE Trans Smart Grid 2023;1. http://dx.doi.org/10.1109/TSG.2023.3257040.

[19] Qian T, Shao C, Li X, Wang X, Shahidehpour M. Enhanced coordinated operations of electric power and transportation networks via EV charging services. IEEE Trans Smart Grid 2020;11(4):3019–30. http://dx.doi.org/10.1109/TSG.2020.2969650.

[20] Geng L, Lu Z, He L, Zhang J, Li X, Guo X. Smart charging management system for electric vehicles in coupled transportation and power distribution systems. Energy 2019;189:116275. http://dx.doi.org/10.1016/j.energy.2019.116275, URL https://www.sciencedirect.com/science/article/pii/S036054421931970X.

[21] Yuan Q, Ye Y, Tang Y, Liu X, Tian Q. Low carbon electric vehicle charging coordination in coupled transportation and power networks. IEEE Trans Ind Appl 2023;59(2):2162–72. http://dx.doi.org/10.1109/TIA.2022.3230014.

[22] Xie S, Xu Y, Zheng X. On dynamic network equilibrium of a coupled power and transportation network. IEEE Trans Smart Grid 2022;13(2):1398–411. http://dx.doi.org/10.1109/TSG.2021.3130384.

[23] Wei W, Mei S, Wu L, Shahidehpour M, Fang Y. Optimal traffic-power flow in urban electrified transportation networks. IEEE Trans Smart Grid 2017;8(1):84–95. http://dx.doi.org/10.1109/TSG.2016.2612239.

[24] Liu X, Soh CB, Zhao T, Wang P. Stochastic scheduling of mobile energy storage in coupled distribution and transportation networks for conversion capacity enhancement. IEEE Trans Smart Grid 2021;12(1):117–30. http://dx.doi.org/10.1109/TSG.2020.3015338.

[25] Sun X, Chen Z, Yin Y. Integrated planning of static and dynamic charging infrastructure for electric vehicles. Transp Res D 2020;83:102331. http://dx.doi.org/10.1016/j.trd.2020.102331, URL https://www.sciencedirect.com/science/article/pii/S1361920919304146.

[26] Nasr Esfahani H, Liu Z, Song Z. Optimal pricing for bidirectional wireless charging lanes in coupled transportation and power networks. Transp Res C 2022;135:103419. http://dx.doi.org/10.1016/j.trc.2021.103419, URL https://www.sciencedirect.com/science/article/pii/S0968090X21004137.

[27] Lv S, Wei Z, Sun G, Chen S, Zang H. Optimal power and semi-dynamic traffic flow in urban electrified transportation networks. IEEE Trans Smart Grid 2020;11(3):1854–65. http://dx.doi.org/10.1109/TSG.2019.2943912.

[28] Qu Z, Xu C, Yang F, Ling F, Pirouzi S. Market clearing price-based energy management of grid-connected renewable energy hubs including flexible sources according to thermal, hydrogen, and compressed air storage systems. J Energy Storage 2023;69:107981. http://dx.doi.org/10.1016/j.est.2023.107981, URL https://www.sciencedirect.com/science/article/pii/S2352152X23013786.

[29] Zhang X, Yu X, Ye X, Pirouzi S. Economic energy management of networked flexi-renewable energy hubs according to uncertainty modeling by the unscented transformation method. Energy 2023;278:128054. http://dx.doi.org/10.1016/j.energy.2023.128054, URL https://www.sciencedirect.com/science/article/pii/S0360544223014482.

[30] Norouzi M, Aghaei J, Niknam T, Pirouzi S, Lehtonen M. Bi-level fuzzy stochastic-robust model for flexibility valorizing of renewable networked microgrids. Sustain Energy Grids Netw 2022;31:100684. http://dx.doi.org/10.1016/j.segan.2022.100684, URL https://www.sciencedirect.com/science/article/pii/S2352467722000431.

[31] Wang L, Kwon J, Schulz N, Zhou Z. Evaluation of aggregated EV flexibility with TSO-DSO coordination. IEEE Trans Sustain Energy 2022;13(4):2304–15. http://dx.doi.org/10.1109/TSTE.2022.3190199.

[32] Hoque MM, Khorasany M, Razzaghi R, Jalili M, Wang H. Network-aware coordination of aggregated electric vehicles considering charge–discharge flexibility. IEEE Trans Smart Grid 2023;14(3):2125–39. http://dx.doi.org/10.1109/TSG.2022.3204761.

[33] Homaee O, Najafi A, Jasinski M, Tsaousoglou G, Leonowicz Z. Coordination of neighboring active distribution networks under electricity price uncertainty using distributed robust bi-level programming. IEEE Trans Sustain Energy 2023;14(1):325–38. http://dx.doi.org/10.1109/TSTE.2022.3212004.

[34] Zhang J, Che L, Wan X, Shahidehpour M. Distributed hierarchical coordination of networked charging stations based on peer-to-peer trading and EV charging flexibility quantification. IEEE Trans Power Syst 2022;37(4):2961–75. http://dx.doi.org/10.1109/TPWRS.2021.3123351.

[35] Norouzi M, Aghaei J, Pirouzi S, Niknam T, Fotuhi-Firuzabad M. Flexibility pricing of integrated unit of electric spring and EVs parking in microgrids. Energy 2022;239:122080. http://dx.doi.org/10.1016/j.energy.2021.122080, URL https://www.sciencedirect.com/science/article/pii/S0360544221023288.

[36] He F, Yin Y, Lawphongpanich S. Network equilibrium models with battery electric vehicles. Transp Res B 2014;67:306–19. http://dx.doi.org/10.1016/j.trb.2014.05.010, URL https://www.sciencedirect.com/science/article/pii/S0191261514000915.

[37] Wang S, Chen S, Ge L, Wu L. Distributed generation hosting capacity evaluation for distribution systems considering the robust optimal operation of OLTC and SVC. IEEE Trans Sustain Energy 2016;7(3):1111–23. http://dx.doi.org/10.1109/TSTE.2016.2529627.

[38] Baran ME, Wu FF. Network reconfiguration in distribution systems for loss reduction and load balancing. IEEE Trans Power Deliv 1989;4(2):1401–7. http://dx.doi.org/10.1109/61.25627.

[39] Low SH. Convex relaxation of optimal power flow—Part II: Exactness. IEEE Trans Control Netw Syst 2014;1(2):177–89.

[40] Nagarajan H, Lu M, Wang S, Bent R, Sundar K. An adaptive, multivariate partitioning algorithm for global optimization of nonconvex programs. J Global Optim 2019;74:639–75. http://dx.doi.org/10.1007/s10898-018-00734-1, URL https://www.sciencedirect.com/science/article/pii/S0191261514000915.

[41] Carrion M, Arroyo JM, Conejo AJ. A bilevel stochastic programming approach for retailer futures market trading. IEEE Trans Power Syst 2009;24(3):1446–56. http://dx.doi.org/10.1109/TPWRS.2009.2019777.

[42] Homaee O, Zakariazadeh A, Jadid S. Real-time voltage control algorithm with switched capacitors in smart distribution system in presence of renewable generations. Int J Electr Power Energy Syst 2014;54:187–97. http://dx.doi.org/10.1016/j.ijepes.2013.07.010.

[43] Oskouei MZ, Mohammadi-Ivatloo B, Abapour M, Shafiee M, Anvari-Moghaddam A. Strategic operation of a virtual energy hub with the provision of advanced ancillary services in industrial parks. IEEE Trans Sustain Energy 2021;12(4):2062–73. http://dx.doi.org/10.1109/TSTE.2021.3079256.

[44] Agriculture ND. North Dakota agriculture weather network, Available at: http://ndawn.ndsu.nodak.edu/wind-speeds.html. [Accessed 18 April 2022].

[45] NYISO. NewYork independent system operator, Available at: http://www.nyiso.com.

[46] Pineda S, Conejo AJ. Scenario reduction for risk-averse electricity trading. IET Gener Transm Distrib 2010;4(6):694–705. http://dx.doi.org/10.1049/iet-gtd.2009.0376, Cited by: 53. URL https://www.scopus.com/inward/record.uri?eid=2-s2.0-77954158368&doi=10.1049%2fiet-gtd.2009.0376&partnerID=40&md5=1b48b8ca39818a7f2f202e201eceddbc.